Environ Sci Pollut Res (2012) 19:2159–2171
DOI 10.1007/s11356-011-0715-x

RESEARCH ARTICLE

# Radiative effects of aerosols over Indo-Gangetic plain: environmental (urban vs. rural) and seasonal variations

**S. Ramachandran · Sumita Kedia**

Received: 12 August 2011 / Accepted: 20 December 2011 / Published online: 10 January 2012


**Abstract** Aerosol radiative effects over two environmentally distinct locations, Kanpur (urban site) and Gandhi College (rural location) in the Indo-Gangetic plain (IGP), a regional aerosol hot spot, utilizing the measured optical and physical characteristics of aerosols, an aerosol optical properties model and a radiative transfer model, are examined. Shortwave aerosol radiative forcing (ARF) at the top of the atmosphere (TOA) is $<-12$ W m$^{-2}$ over Kanpur and Gandhi College. ARF at the surface is $\geq -30$ W m$^{-2}$. Atmospheric warming is maximum during premonsoon ($>30$ W m$^{-2}$). Shortwave atmospheric heating due to aerosols is $>0.4$ K/day over IGP and peaks during premonsoon at $>0.6$ K/day due to lower single scattering albedo (SSA) and higher surface albedo. TOA forcing is always less negative over Kanpur when compared to Gandhi College due to lower surface albedo except in postmonsoon owing to higher SSA. This happens as TOA forcing depends on SSA and surface albedo in addition to aerosol optical depth. The magnitude of longwave forcing and atmospheric cooling in an absolute sense is significantly small and contributes only about 20% or less to the net (shortwave + longwave) forcing. Aerosol radiative effects over these two locations, despite differences in aerosol characteristics, are similar, thus confirming that aerosols and their radiative influence get transported due to circulation. ARF over Kanpur and Gandhi College is an order of magnitude higher when compared to greenhouse gas forcing. A large reduction in surface reaching solar irradiance accompanied by large atmospheric warming can have implications on precipitation and hydrological cycle, and these aerosol radiative effects should be included while performing regional-scale aerosol climate assessments.

**Keywords** Indo-Gangetic plain · Aerosol forcing · Shortwave · Longwave · Urban *vs.* Rural · Seasonal · Variations · Comparison

## 1 Introduction

Aerosols are a major atmospheric (ATM) component and influence the transfer of radiative energy and the conversion of water vapor into cloud droplets and raindrops. Despite the worldwide attention and several studies on the radiative effects of aerosols, they remain one of the largest sources of uncertainty in estimating climate forcing (Solomon et al. 2007). The uncertainty in aerosol radiative effects mainly arises due to the lack of reliable measurements on the spatial and temporal distribution of aerosols. The sources of aerosols include natural and anthropogenic and possess distinct characteristics and size distributions. The fine mode aerosols over urban, industrialized and densely populated regions arise mostly from gas to particle conversion and combustion which are mainly anthropogenic, while coarse mode aerosols such as windblown mineral dust and sea salt particles originate from

Responsible editor: Euripides Stephanou

S. Ramachandran · S. Kedia (✉)
Space and Atmospheric Sciences Division, Physical Research Laboratory, Navrangpura, Ahmedabad, Gujarat 380009, India
e-mail: sumita@prl.res.in

S. Ramachandran
e-mail: ram@prl.res.in

natural sources. Over India, the meteorology, sources of aerosols and their emissions are found to be different (Ramachandran and Cherian 2008), and different regions were found influenced by aerosols produced from both natural and anthropogenic sources. Since the optical, physical and chemical characteristics of aerosols produced from natural sources are distinct from those emitted from manmade sources, the radiative effects of aerosols also vary. Indo-Gangetic plain (IGP) is one such region, where both natural and anthropogenic sources contribute to ambient aerosols throughout the year. This region is bordered by the Himalayas to the north and Vindhyan Satpura ranges to the south. IGP is a densely populated region over which emissions from biomass burning, industries, power plants and vehicles contribute dominantly to aerosols throughout the year (Singh et al. 2004; Dey and Tripathi 2008; Ramachandran and Cherian 2008). Aerosol optical depths (AODs) are found to be higher over this region when compared to the other regions in India throughout the year (Ramachandran and Cherian 2008).

Seasonal variability in aerosol characteristics and radiative effects have been studied over Kanpur in IGP, an Aerosol Robotic Network (AERONET) station (Singh et al. 2004; Dey and Tripathi 2008). Kanpur is an urban, industrial city with a population of more than four million (Singh et al. 2004). AODs over Kanpur were found to show a pronounced seasonal influence with maximum dust loading during premonsoon (Singh et al. 2004). Single scattering albedo values were lower during winter due to the dominance of absorbing aerosols (Singh et al. 2004). Aerosols were found to produce a large negative forcing exceeding $-20\ \mathrm{W\ m^{-2}}$ during the year with a peak at premonsoon; the peak in surface (SFC) aerosol radiative forcing (ARF) during premonsoon was attributed to the presence of transported natural dust which gets added to manmade pollution (Dey and Tripathi 2008). Gandhi College, a relatively new AERONET station, is a rural village location in Ganga basin, southeast of Kanpur. Gandhi College is influenced by a mixture of rural and urban aerosol emissions as it is situated downwind of major urban centers, such as Delhi, Lucknow and Kanpur (Fig. 1).

Aerosol characteristics (aerosol optical depth, single scattering albedo and asymmetry parameter) obtained over Kanpur and Gandhi College and their seasonal variations during 2006–2008 form the inputs for this


**Fig. 1** The study locations over the Indo-Gangetic Plain—Kanpur and Gandhi College are shown on a Google image, in addition to a few major cities in India. Latitude, longitude and altitude of the locations above mean sea level in metres are given

study. Kanpur (Fig. 1) is found to be dominated by coarse mode natural aerosols, while fine mode aerosols from the mixture of biomass (rural) and fossil fuel (urban) emissions (Solomon et al. 2007) are expected to dominate the rural location Gandhi College (Fig. 1). The differences in the abundance of aerosols of different sizes can affect the aerosol radiative forcing differently in the shortwave and longwave regions. The objective of this study is to examine the spatiotemporal variations in aerosol radiative effects over two distinctly different environments, separated by about 300 km, but governed by different types of aerosols produced from different sources. Srivastava et al. (2011) studied the aerosol characteristics and shortwave radiative effects utilizing the AERONET data over Kanpur and Gandhi College corresponding to April–May–June 2009. In the present study, for the first time, we compare and contrast (a) the model derived aerosol radiative forcing and AERONET retrieved aerosol radiative forcing and (b) the seasonal variation in aerosol radiative effects in the shortwave and longwave regions on a regional scale over Kanpur and Gandhi College in IGP and discuss the possible climate implications.

## 2 Meteorological and atmospheric parameters of study locations

Temperatures are colder and the atmosphere is dry during winter (December–January–February) (Table 1) over IGP. In premonsoon (March–April–May) temperatures increase and relative humidity (RH) differ only slightly when compared to winter. During monsoon (June–July–August–September), both temperature and RH are high; however, increase in RH is more significant (Table 1). During postmonsoon (October–November), temperatures are similar to monsoon while RH reduces. The seasonal mean meteorological and atmospheric parameters are calculated using the daily mean values from January 2006 to December 2008. On the basis of meteorology, the results are discussed as function of four major seasons of winter, premonsoon, monsoon and postmonsoon.

## 3 Estimation of aerosol radiative forcing: aerosol inputs, atmospheric parameters and methodology

*Aerosol inputs* In the current study, spectral AERONET Sun/sky scanning radiometer measured quality assured and cloud screened level 2.0 monthly mean AODs at 0.34, 0.38, 0.44, 0.50, 0.67, 0.87 and 1.02 μm, single scattering albedo (SSA) and asymmetry parameter ($g$) at 0.44, 0.67, 0.87 and 1.02 μm from January 2006 to December 2008 at Kanpur and Gandhi College are utilized. The uncertainty in AERONET retrieved AODs is less than ±0.02 in the 0.34–1.02 μm wavelength range (Dubovik and King 2000). The error in SSA is estimated to be 0.03 when AOD at 0.44 μm is >0.2 and becomes higher (0.05–0.07) when AOD is ≤0.2 (Dubovik and King 2000). Uncertainty in asymmetry parameter is reported to be in the range of 3–5% (Andrews et al. 2006).

Seasonal and annual mean differences in AOD (0.5 μm), Ångström wavelength exponent ($\alpha$), fine mode fraction (FMF; 0.5 μm), SSA and $g$ at 0.55 μm for Kanpur and Gandhi College are given in Table 2. $\alpha$ is derived following Ångström power law curve ($\tau = \beta\lambda^{-\alpha}$, where $\tau$ is AOD). The $\alpha$ values are estimated for an individual data set comprising of AODs in the 0.34–0.87 μm wavelength range by least squares fitting AOD against wavelength on a log–log plot. The wavelength exponent $\alpha$ depends on the size distribution of aerosols, and $\beta$ is directly proportional to the columnar aerosol content. Higher $\alpha$ signifies an increase in the concentration of submicron aerosols and a decrease in the concentration of larger particles whereas lower value of $\alpha$ indicates a larger abundance of supermicron particles.

**Table 1** Seasonal mean meteorological variables (temperature (degree Celsius) and relative humidity (in percent)) and atmospheric parameters (columnar water vapor (centimetres) and ozone (Dobson unit) over Kanpur and Gandhi College during 2006–2008 along with ±1$\sigma$ deviation from the mean

| Seasons | Temperature (°C) | Relative humidity (%) | Columnar water vapor (cm) | Columnar ozone (DU) | Surface reflectance (0.555 μm) |
|---|---|---|---|---|---|
| Kanpur | | | | | |
| Winter | 20.0 ± 1.8 | 41 ± 5 | 1.5 ± 0.5 | 256.9 ± 14.4 | 0.099 ± 0.007 |
| Premonsoon | 29.2 ± 0.2 | 33 ± 2 | 2.3 ± 0.8 | 280.6 ± 11.4 | 0.132 ± 0.023 |
| Monsoon | 28.6 ± 0.2 | 80 ± 1 | 5.0 ± 1.1 | 274.6 ± 7.2 | 0.118 ± 0.024 |
| Postmonsoon | 23.8 ± 0.4 | 58 ± 2 | 2.2 ± 0.6 | 262.2 ± 8.6 | 0.113 ± 0.007 |
| Gandhi College | | | | | |
| Winter | 22.9 ± 1.7 | 41 ± 6 | 1.8 ± 0.5 | 255.2 ± 13.0 | 0.083 ± 0.012 |
| Premonsoon | 30.5 ± 0.4 | 39 ± 2 | 2.8 ± 1.0 | 279.6 ± 11.4 | 0.110 ± 0.028 |
| Monsoon | 28.0 ± 0.5 | 88 ± 2 | 5.7 ± 0.8 | 272.9 ± 7.4 | 0.095 ± 0.048 |
| Postmonsoon | 24.3 ± 0.6 | 72 ± 2 | 2.8 ± 0.8 | 260.9 ± 8.5 | 0.080 ± 0.013 |

**Table 2** Seasonal and annual mean variation in AOD, Ångström wavelength exponent ($\alpha$), FMF, SSA and asymmetry parameter over Kanpur and Gandhi College

| Seasons | AOD (0.5 μm) | $\alpha$ (0.34–0.87 μm) | FMF (0.5 μm) | SSA (0.55 μm) | $g$ (0.55 μm) |
|---|---|---|---|---|---|
| Kanpur | | | | | |
| Winter | 0.69 ± 0.19 | 1.14 ± 0.11 | 0.85 ± 0.14 | 0.89 ± 0.00 | 0.68 ± 0.01 |
| Premonsoon | 0.55 ± 0.12 | 0.75 ± 0.18 | 0.44 ± 0.08 | 0.86 ± 0.03 | 0.69 ± 0.02 |
| Monsoon | 0.50 ± 0.15 | 0.89 ± 0.21 | 0.52 ± 0.15 | 0.89 ± 0.01 | 0.69 ± 0.01 |
| Postmonsoon | 0.75 ± 0.34 | 1.14 ± 0.00 | 0.82 ± 0.19 | 0.90 ± 0.00 | 0.68 ± 0.00 |
| Annual | 0.62 ± 0.11 | 0.96 ± 0.22 | 0.63 ± 0.22 | 0.88 ± 0.02 | 0.68 ± 0.01 |
| Gandhi College | | | | | |
| Winter | 0.74 ± 0.13 | 1.30 ± 0.01 | 0.94 ± 0.01 | 0.89 ± 0.01 | 0.67 ± 0.01 |
| Premonsoon | 0.61 ± 0.19 | 0.91 ± 0.15 | 0.56 ± 0.09 | 0.88 ± 0.01 | 0.69 ± 0.01 |
| Monsoon | 0.59 ± 0.15 | 1.07 ± 0.21 | 0.66 ± 0.15 | 0.90 ± 0.00 | 0.70 ± 0.00 |
| Postmonsoon | 0.70 ± 0.16 | 1.26 ± 0.06 | 0.90 ± 0.05 | 0.88 ± 0.03 | 0.68 ± 0.00 |
| Annual | 0.66 ± 0.07 | 1.10 ± 0.21 | 0.73 ± 0.18 | 0.89 ± 0.02 | 0.69 ± 0.01 |

$\alpha$ is calculated from AODs in the 0.34–0.87 μm wavelength region
*AOD* aerosol optical depth, *FMF* fine mode fraction, *SSA* single scattering albedo

FMF is defined as the ratio of the fine/accumulation mode aerosol optical depth (0.1–1.0 μm) to the total aerosol optical depth (0.01–10.0 μm). AOD, $\alpha$ and FMF exhibit large seasonal variation over Kanpur and Gandhi College (Table 2). AODs decrease from winter to monsoon. $\alpha$ and FMF are higher in Gandhi College when compared to Kanpur confirming the higher abundance of fine mode aerosols over Gandhi College throughout the year. SSA and $g$ at 0.55 μm do not exhibit significant seasonal variation and are more or less comparable over Kanpur and Gandhi College.

*Atmospheric parameters* Monthly mean atmospheric profiles of temperature and pressure corresponding to Kanpur and Gandhi College from NCEP reanalysis (http://www.cdc.noaa.gov) are used to construct the seasonal means and are used in the present study. Columnar water vapor is higher during monsoon and is marginally higher over Gandhi College (Table 1). Water vapor is ≤4 cm during the rest of the year (Table 1) consistent with the results reported earlier over Kanpur (Singh et al. 2004). Ozone (http://gdata1.sci.gsfc.nasa.gov) shows a premonsoon (spring) high quite consistent with the ozone variation in the tropics (Table 1). Columnar ozone is ≥260 Dobson units (DU) over Kanpur and Gandhi College during premonsoon, monsoon and postmonsoon. Though surface reflectance is not an aerosol property, it plays an important role in determining the magnitude and sign of aerosol radiative forcing (Solomon et al. 2007). In the present study, surface reflectance measured by MODIS on board Terra and Aqua satellites (8-Day, Level 3 Global 500 m ISIN Grid product, MOD09A1 (Terra) and MYD09A1 (Aqua)) at seven wavelength bands centered at 0.469, 0.555, 0.645, 0.859, 1.24, 1.64 and 2.13 μm are utilized to calculate the Terra–Aqua mean surface reflectance value over the study locations. The monthly mean surface reflectance (along with $\pm 1\sigma$) obtained from MODIS are used to estimate the seasonal mean surface reflectance over Kanpur and Gandhi College at seven different wavelength bands during 2006–2008. Surface reflectance values at 0.555 μm over Kanpur and Gandhi College as function of season are given in Table 1 as example (Table 1). The surface reflectance values are higher during premonsoon and monsoon. The surface reflectance data from MODIS are available only at seven wavelength bands. However, for the estimation of aerosol radiative forcing, surface reflectance values as a function of wavelength for the entire shortwave and longwave spectral range are required. Therefore, the spectral surface reflectance is produced by combining sand, vegetation and water in certain proportion such that the resultant spectrum of surface reflectance is close to the observed values from MODIS (Ramachandran et al. 2006) and are used in aerosol radiative forcing estimates. Further, by appropriately varying the percentage of the above three surface types, monthly mean spectral surface reflectances over Kanpur and Gandhi College have been calculated, which are then used to obtain seasonal mean values.

*Methodology* Optical properties of aerosols and clouds model (Hess et al. 1998) is used in conjunction with the measured aerosol parameters in the present study. The required aerosol parameters (AOD, SSA and $g$) in the shortwave and longwave regions are derived by varying the aerosol components that contributed to the aerosol properties over Kanpur and Gandhi College. The aerosol properties are calculated on the basis of the microphysical data (size distribution and spectral refractive index) assuming aerosols as spherical particles and externally mixed. Optical properties of aerosols and clouds (OPAC) outputs the aerosol parameters at eight different relative humidity (0%, 50%, 70%, 80%, 90%, 95%, 98% and 99%) con-

ditions (Hess et al. 1998), as some of the aerosol components are hygroscopic. The aerosol components that could contribute to the aerosol distribution over the two study locations based on the aerosol source regions, transport pathways, wind patterns, meteorology and a few earlier studies (Singh et al. 2004; Dey and Tripathi 2008) are found to be water soluble, insoluble, black carbon, sea salt and mineral dust. In the present study, the number concentrations of the above aerosol components are varied to match the measured aerosol properties over the study locations, and aerosol parameters (AOD, SSA and $g$) corresponding to the monthly mean RH are obtained. The number concentrations of different aerosol species are varied until the following conditions are satisfied: (1) The root mean square (rms) error between the measured and estimated AOD, SSA and $g$ spectra is <0.03, thus constraining the rms difference to within the uncertainty of the measured parameters, and (2) Ångström wavelength exponent $\alpha$ determined from the measured AODs in the 0.34–1.02 μm wavelength range are consistent with model derived $\alpha$ values. Aerosol properties (AOD, SSA and $g$) calculated as above for all the months during 2006–2008 are further used for determining the seasonal mean.

Santa Barbara DISORT Atmospheric Radiative Transfer (SBDART) (Ricchiazzi et al. 1998) model is used to estimate ARF. The discrete ordinate method provides a numerically stable algorithm to solve the equations of plane-parallel radiative transfer in a vertically inhomogeneous atmosphere. The intensity of both scattered and thermally emitted radiations can be computed at different heights and directions. SBDART computes aerosol radiative forcing in the shortwave (0.2–4.0 μm) and longwave (4.0–40.0 μm) regions. The radiative fluxes are computed for clear sky conditions in the presence of aerosols and for aerosol free atmosphere in both the wavelength regimes and the difference between the net (down-up) radiative fluxes with and without aerosols is termed as the aerosol radiative forcing in the shortwave and longwave regions. The radiative fluxes are computed using eight radiation streams at 1-h interval for a range of solar zenith angles and 24-h averages are obtained for each month, which are then used to construct the seasonal means and presented. SBDART estimated direct and diffuse irradiances were found to vary by <2% when compared to the measured irradiances at the surface (Michalsky et al. 2006). The difference between the radiative forcing at the top of the atmosphere (TOA; which is 100 km in this case) and surface is defined as the ATM forcing. If ATM forcing is positive, the aerosols contribute to a net gain of radiative flux to the atmosphere leading to a warming, while a negative ATM forcing indicates a net loss and thereby cooling.

The absorption and emission processes in the longwave at different altitudes in the atmosphere, when integrated over all the wavelengths, can warm (gain of radiative energy) or cool (loss of radiative energy) (Ramaswamy 2002) the atmosphere; in contrast, absorption in the shortwave by aerosols always warms the atmosphere. The amount of energy absorbed (and/or scattered in case of longwave) by the aerosols is referred to as the atmospheric heating rate and is expressed in kelvin per day as

$$\frac{\partial T}{\partial t} = \frac{\mathrm{g}}{c_{\mathrm{p}}}\left[\frac{\Delta F_{\mathrm{ATM}}}{\Delta P}\right] \quad (1)$$

where $\partial T/\partial t$ is the heating rate (kelvin per day), $g$ is the acceleration due to gravity, $c_{\mathrm{p}}$ is the specific heat capacity of air at constant pressure and $P$ is the atmospheric pressure (Liou 1980). The heating rates are calculated separately for shortwave and longwave regions, by inserting the appropriate ATM forcing for the respective wavelength regions.

The atmospheric/planetary boundary layer height plays an important role in the columnar aerosol concentration as it strongly affects the vertical mixing of aerosols (Stull 1988). During winter and postmonsoon, atmospheric boundary layer height remains low due to less insolation at the Earth's surface and results in an inversion layer which opposes vertical mixing of aerosols. In contrast, during premonsoon and monsoon, the height of boundary layer increases when the solar insolation increases as also reflected in the higher surface temperature during these seasons (Table 1). A comparison of measured profiles of aerosol extinction coefficients and columnar aerosol optical depths revealed that aerosol extinction in the surface 5 km altitude region contributes >98% to the columnar aerosol optical depth during the year (Ramachandran and Kedia 2010). Therefore, ΔP (in Eq. 1) is considered as 454 hPa which is equal to the pressure difference between the surface and 5 km in the tropics. The relative standard error in radiative forcing and heating rate reported in the study, taking into account the uncertainties in aerosol input parameters, additional inputs and flux estimates, is found to be <15%.

### 3.1 Comparison of aerosol radiative forcing: AERONET and SBDART

Aerosol radiative forcing estimated using the approach described above is compared with AERONET directly as point values available at a particular time during the

day in Kanpur and Gandhi College in Table 3. Aerosol properties retrieved in AERONET are used in calculating the solar broad band fluxes in the spectral range from 0.2 to 4.0 μm. The flux simulation relies on the retrieved real and imaginary parts of refractive index. The spectral integration uses real and imaginary parts of the refractive index that are either extrapolated or interpolated using the values of refractive index retrieved at AERONET wavelengths (Dubovik and King 2000). In a similar manner, the spectral dependence of surface reflectance is interpolated/extrapolated from surface albedo values assumed during retrieval at the wavelengths of AERONET. The surface reflectance for land sites of AERONET is approximated by bidirectional reflectance distribution function adapted from the MODIS Ecotype models (Dubovik and King 2000). The radiative transfer calculations for gaseous absorption is done using global atmospheric model (Dubuisson et al. 1996). The standard deviation for error in AERONET sky radiance measurements is assumed to be 5% (Dubovik and King 2000). Aerosol radiative forcing retrieved using OPAC and SBDART models compares quite well with AERONET retrieved values over Kanpur and Gandhi College (Table 3) despite the different methodologies adopted. Regression lines between SBDART estimated radiative forcing and AERONET radiative forcing at TOA and SFC yielded $R^2 > 0.96$. Thus, these results and comparison confirm that the modeling approach adopted to estimate aerosol properties and the resultant radiative forcing is robust, and the problem of retrieval of spectral aerosol properties is constrained well enough for the solution of the inversion to be unique.

### 3.2 Influence of vertical distribution of aerosols on radiative forcing

Vertical distribution of aerosols is another important input required to estimate aerosol radiative forcing, as lack of information on the vertical distribution can introduce uncertainty in aerosol radiative forcing as a function of altitude (Solomon et al. 2007). In this study, the aerosols are distributed in the atmosphere on the basis of scale height, which is 8 km for continental locations. Our earlier study over another continental location revealed that aerosol radiative forcing at the top of the atmosphere, surface and atmosphere and the heating rates obtained with and without including vertical distribution of aerosols exhibit negligible differences (Ramachandran and Kedia 2010). Thus, ascertaining that the net energy content trapped in the atmosphere remains the same with and without vertical profiles, but only its vertical distribution varies. The objective of the present study is to estimate the net aerosol radiative forcing at the top of the atmosphere, surface and in the atmosphere, and therefore, non-inclusion of the vertical distribution of aerosols is not expected to modify the outcomes and conclusions.

## 4 Results and discussion

### 4.1 Aerosol radiative forcing and heating rate

Figure 2 shows the seasonal mean shortwave ARF over Kanpur and Gandhi College at TOA, SFC and ATM. TOA forcing is negative and is $<-12$ W m$^{-2}$ throughout the year at Kanpur and Gandhi College; TOA forcing is least negative during premonsoon season over both the locations. SFC forcing is $\geq -30$ W m$^{-2}$ (Fig. 2). ATM forcing is maximum during premonsoon, as the difference between TOA and SFC forcing is maximum during premonsoon. ARF is less sensitive to changes in asymmetry parameter (Mishchenko et al. 1997); however, the seasonal changes in $g$ over Kanpur and Gandhi College are small (Table 2). Seasonal variation in SSA and $g$ is less in the mid-visible wavelengths (Table 2) when compared to AODs. SSA and $g$ decrease as a function of wavelength when fine mode aerosols from fossil fuel and biomass burning dominate, while SSA and $g$ can remain more or less the same or increase as wavelength increases when coarse mode

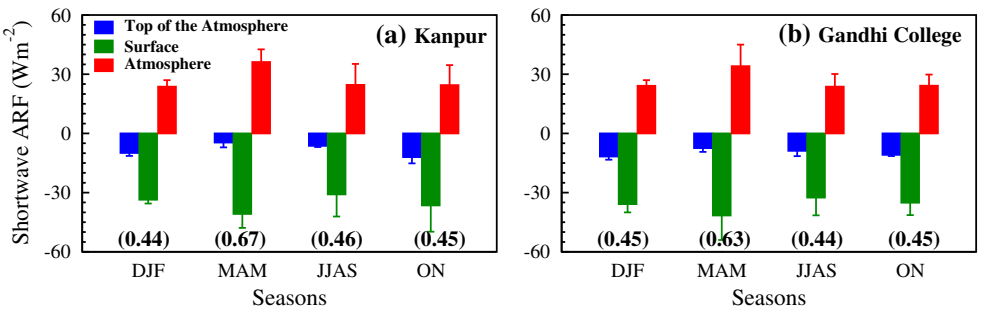


**Fig. 2** Seasonal variation in shortwave aerosol radiative forcing (*ARF*) at the top of the atmosphere, surface and in the atmosphere estimated for **a** Kanpur and **b** Gandhi College. *Vertical bars* indicate $\pm 1\sigma$ variation from the mean. The solar heating rates (kelvin per day) are given in *brackets*

**Table 3** Comparison of aerosol parameters (AOD at 0.5 μm, SSA at 0.55 μm and asymmetry parameter (*g*) at 0.55 μm obtained in Kanpur and Gandhi College from AERONET with model (OPAC) retrieved values during different days of the year (point values at particular time)

| Date | Time (GMT) | Aerosol parameters | | | | | | Aerosol radiative forcing (W $m^{-2}$) | | | |
|---|---|---|---|---|---|---|---|---|---|---|---|
| | | AERONET | | | MODEL (OPAC) | | | AERONET | | MODEL (SBDART) | |
| | | AOD | SSA | *g* | AOD | SSA | *g* | TOA | SFC | TOA | SFC |
| Kanpur | | | | | | | | | | | |
| 1 Jan 2006 | 10.0 | 0.68 | 0.87 | 0.67 | 0.66 | 0.87 | 0.65 | −33.8 | −110.7 | −30.2 | −100.3 |
| 1 Feb 2006 | 10.0 | 0.79 | 0.86 | 0.69 | 0.78 | 0.86 | 0.65 | −30.1 | −137.8 | −28.1 | −135.0 |
| 4 Mar 2006 | 10.0 | 0.41 | 0.85 | 0.69 | 0.44 | 0.86 | 0.67 | −15.4 | −85.1 | −14.6 | −87.5 |
| 18 Apr 2006 | 12.0 | 0.59 | 0.91 | 0.67 | 0.62 | 0.91 | 0.66 | −26.3 | −61.4 | −28.8 | −67.4 |
| 1 May 2006 | 11.0 | 0.86 | 0.90 | 0.72 | 0.90 | 0.92 | 0.69 | −43.9 | −129.9 | −39.8 | −137.2 |
| 4 Jun 2008 | 12.0 | 1.13 | 0.91 | 0.68 | 1.12 | 0.90 | 0.68 | −31.5 | −106.4 | −34.2 | −113.3 |
| 3 Sep 2006 | 12.0 | 0.38 | 0.90 | 0.71 | 0.40 | 0.87 | 0.67 | −15.8 | −51.6 | −16.9 | −50.1 |
| 4 Oct 2006 | 10.0 | 0.47 | 0.86 | 0.66 | 0.50 | 0.90 | 0.67 | −23.1 | −84.6 | −23.6 | −83.9 |
| 12 Nov 2006 | 10.0 | 1.06 | 0.90 | 0.79 | 1.02 | 0.92 | 0.65 | −41.6 | −117.5 | −45.7 | −124.2 |
| 13 Dec 2007 | 10.0 | 1.11 | 0.92 | 0.71 | 1.07 | 0.90 | 0.67 | −44.6 | −144.0 | −42.2 | −137.5 |
| Gandhi College | | | | | | | | | | | |
| 5 Jan 2007 | 10.0 | 0.49 | 0.89 | 0.65 | 0.48 | 0.90 | 0.65 | −28.4 | −74.0 | −27.1 | −72.3 |
| 4 Mar 2007 | 10.0 | 0.37 | 0.90 | 0.64 | 0.40 | 0.91 | 0.65 | −22.3 | −66.5 | −22.6 | −65.6 |
| 20 Apr 2006 | 10.0 | 0.45 | 0.91 | 0.67 | 0.49 | 0.93 | 0.67 | −23.4 | −75.4 | −22.5 | −76.1 |
| 1 May 2006 | 10.0 | 0.85 | 0.87 | 0.69 | 0.85 | 0.89 | 0.67 | −23.8 | −152.5 | −26.0 | −152.9 |
| 10 Jun 2006 | 10.0 | 0.62 | 0.91 | 0.70 | 0.65 | 0.93 | 0.68 | −28.0 | −98.4 | −26.0 | −100.6 |
| 28 Sep 2006 | 10.0 | 0.57 | 0.92 | 0.71 | 0.57 | 0.92 | 0.68 | −26.5 | −76.9 | −27.6 | −80.1 |
| 3 Oct 2006 | 10.0 | 0.62 | 0.94 | 0.68 | 0.63 | 0.94 | 0.68 | −36.3 | −77.9 | −35.4 | −78.0 |
| 6 Nov 2006 | 10.0 | 1.10 | 0.88 | 0.68 | 1.05 | 0.89 | 0.66 | −37.2 | −125.7 | −40.5 | −125.0 |
| 4 Dec 2006 | 10.0 | 0.64 | 0.84 | 0.68 | 0.61 | 0.83 | 0.64 | −19.8 | −85.1 | −20.1 | −91.9 |

Shortwave aerosol radiative forcing (watts per square metre) provided from AERONET at the TOA and at the SFC for the same times are compared with model (SBDART) estimates

*AOD* aerosol optical depth, *TOA* top of the atmosphere, *SSA* single scattering albedo, *SFC* surface

particles (dust and sea salt) dominate. The changes in SSA and *g* will be more significantly seen in the longer wavelengths when compared to the mid-visible when the aerosol type changes. Singh et al. (2004) also reported that at lower wavelengths, the differences in SSA between dust and finer aerosols were small. Shortwave atmospheric heating rate is higher than 0.40 K/day on seasonal and annual mean scales over Kanpur and Gandhi College (Table 3). The heating rate is highest (>0.6 K/day) during premonsoon over Kanpur and Gandhi College.

Shortwave ARF obtained in this study agrees well with results obtained over Kanpur during 2001–2005 by Dey and Tripathi (2008). Dey and Tripathi (2008) reported that ARF at the surface was the highest during premonsoon (>−30 W $m^{-2}$) when long range transported dust gets added to manmade aerosols, as also seen in the present study. The monthly mean surface forcing over Kanpur and Gandhi College during 2009 were found to be −26.1 and −29.7 W $m^{-2}$ (April), −31.7 and −31.5 W $m^{-2}$ (May 2009) and −29.2 and −31.9 W $m^{-2}$ (June), respectively (Srivastava et al. 2011). Mean AODs at 0.55 μm were found to be in the range of 0.50–0.69 over Kanpur and 0.51–0.77 over Gandhi College, respectively, during April–June 2009 (Srivastava et al. 2011). The respective atmospheric forcing was found to be 19.5, 19.6 and 16.1 W $m^{-2}$ over Kanpur during April, May and June 2009, respectively; the corresponding values were 20.9, 16.0 and 16.6 W $m^{-2}$ over Gandhi College (Srivastava et al. 2011). The differences in forcing values between the present study and Srivastava et al. (2011) can be attributed to the differences in AOD, SSA and surface albedo values between the two studies.

For the same type of aerosols (meaning same SSA), surface ARF is linearly related to AODs. However, TOA forcing depends on SSA and surface albedo in addition to AODs and can be either positive (lower SSA) or negative (higher SSA), unlike the greenhouse gas forcing which is always positive. TOA forcing can become less negative and/or positive when aerosols with lower SSA are present over high reflecting surfaces (such as continent, desert, snow) (Solomon et al. 2007). The atmospheric forcing can be higher or lower depending on the value of SSA and surface albedo. Aerosol radiative forcing efficiency (ARFE), defined

as the aerosol radiative forcing normalised by the AOD at 0.5 μm, is a useful measure as after being normalised by AOD, aerosol forcing is mainly governed by the internal aerosol optical properties (SSA) and geographical parameters (surface albedo). To delineate the influence of AOD, SSA and surface reflectance on aerosol radiative forcing, ARFE is calculated for continental clean and urban aerosol models for a range of relative humidities and surface albedo (Table 4). Continental clean aerosol model depicts remote continental locations without or with very low anthropogenic influence (Hess et al. 1998). Urban aerosol model represents strong pollution in urban areas. Continental Clean model is made up of water soluble and insoluble aerosols in low number concentrations which is reflected in small AODs (Table 5). Urban aerosol model in addition to the above two aerosol species has absorbing black carbon aerosols in large number; due to the presence of higher number of water soluble and black carbon aerosols which are in fine mode, AODs are high and SSAs are low for urban aerosols when compared to continental clean aerosols. Surface reflectance is high in May when compared to January over Kanpur (Table 4). ARF at TOA is positive for urban aerosols at 0% RH (when SSA is the lowest) in January when surface albedo is lower, but changes sign as SSA increases. In May when surface albedo is higher (Table 4), ARF at TOA is positive for all relative humidities except at 90%. When compared to urban aerosols, the radiative effects of continental clean aerosols are quite small. ARFE is positive and negative at TOA for urban aerosols. ARFE at TOA and SFC are the highest at lower SSA and decrease as SSA increases for a given surface albedo. When SSA is >0.9 (continental clean aerosols), ARFE at TOA and SFC exhibit no significant differences for low and high surface albedos. This suggests that the influence of surface albedo will be more prominent when SSA is <0.9 (urban aerosols). Thus, this sensitivity study clearly illustrates that ARFE at TOA and SFC can exhibit differences depending on the type of aerosols present (low or high SSA) over a given surface.

**Table 4** Surface reflectance at different wavelengths from MODIS satellite data over Kanpur during January and May

| λ | Surface albedo | |
|---|---|---|
| (μm) | January | May |
| 0.469 | 0.054 ± 0.005 | 0.094 ± 0.014 |
| 0.555 | 0.097 ± 0.009 | 0.156 ± 0.022 |
| 0.645 | 0.106 ± 0.011 | 0.182 ± 0.028 |
| 0.859 | 0.245 ± 0.019 | 0.295 ± 0.025 |
| 1.240 | 0.267 ± 0.019 | 0.335 ± 0.029 |
| 1.640 | 0.239 ± 0.018 | 0.334 ± 0.038 |
| 2.130 | 0.173 ± 0.016 | 0.269 ± 0.041 |

ARFE at TOA and SFC exhibit significant seasonal differences over Kanpur and Gandhi College (Table 6). ARFE at TOA is less negative during premonsoon, while ARFE at SFC is the highest (more negative) over both the locations. During premonsoon, SSA is the lowest in both locations (Table 2) and surface reflectance is the highest (Table 1). These results are consistent with the results obtained from the sensitivity study (Table 5). TOA forcing is always less negative over Kanpur owing to lower surface albedo (Table 1) except during postmonsoon (Table 6). TOA forcing is more negative over Kanpur during postmonsoon

**Table 5** Aerosol radiative forcing (watts per square metre) at the TOA and at the SFC and aerosol radiative forcing efficiencies for continental clean and urban aerosol models for a range of relative humidities and for low (January) and high (May) surface albedos

| RH (%) | AOD | SSA | January | | | | May | | | |
|---|---|---|---|---|---|---|---|---|---|---|
| | | | Forcing | | Efficiency | | Forcing | | Efficiency | |
| | | | TOA | SFC | TOA | SFC | TOA | SFC | TOA | SFC |
| | Continental clean | | | | | | | | | |
| 0 | 0.04 | 0.94 | −1.35 | −2.43 | −31.3 | −56.1 | −1.00 | −2.53 | −23.1 | −58.3 |
| 50 | 0.05 | 0.96 | −1.71 | −2.63 | −30.4 | −46.8 | −1.32 | −2.63 | −23.5 | −46.8 |
| 70 | 0.06 | 0.97 | −1.93 | −2.80 | −30.1 | −43.6 | −1.51 | −2.74 | −23.5 | −42.7 |
| 80 | 0.07 | 0.97 | −2.17 | −2.99 | −29.7 | −41.1 | −1.72 | −2.90 | −23.6 | −39.8 |
| 90 | 0.09 | 0.98 | −2.74 | −3.51 | −29.1 | −37.3 | −2.21 | −3.33 | −23.5 | −35.4 |
| | Urban | | | | | | | | | |
| 0 | 0.41 | 0.67 | 1.18 | −39.22 | 2.9 | −95.2 | 8.36 | −50.30 | 20.3 | −122.1 |
| 50 | 0.55 | 0.75 | −1.43 | −41.61 | −2.6 | −75.6 | 5.86 | −52.85 | 10.6 | −96.0 |
| 70 | 0.64 | 0.79 | −2.99 | −43.03 | −4.7 | −67.6 | 4.32 | −54.44 | 6.8 | −85.5 |
| 80 | 0.73 | 0.82 | −4.58 | −44.53 | −6.3 | −61.0 | 2.75 | −56.18 | 3.8 | −77.0 |
| 90 | 0.96 | 0.86 | −8.26 | −48.01 | −8.6 | −50.1 | −1.00 | −60.41 | −1.1 | −63.0 |

AOD at 0.50 μm and SSA at 0.55 μm from Hess et al. (1998) are given
*HR* heating rate, *AOD* aerosol optical depth, *SSA* single scattering albedo, *TOA* top of the atmosphere, *SFC* surface

**Table 6** Seasonal and annual mean shortwave and longwave aerosol radiative forcing (watts per square metre) at the TOA, the SFC and in the ATM, along with HR (kelvin/day) over Kanpur and Gandhi College

| Period | Aerosol radiative forcing | | | | | | | | | |
|---|---|---|---|---|---|---|---|---|---|---|
| | Efficiency | | Shortwave | | | | Longwave | | | |
| | TOA | SFC | TOA | SFC | ATM | HR | TOA | SFC | ATM | HR |
| Kanpur | | | | | | | | | | |
| Winter | −14.80 | −51.85 | −9.94 | −33.64 | 23.70 | 0.44 | 1.76 | 4.38 | −2.62 | −0.05 |
| Premonsoon | −8.20 | −74.72 | −4.61 | −40.76 | 36.15 | 0.67 | 4.52 | 8.36 | −3.84 | −0.07 |
| Monsoon | −13.16 | −61.48 | −6.34 | −30.92 | 24.58 | 0.46 | 2.91 | 3.63 | −0.72 | −0.01 |
| Postmonsoon | −16.90 | −50.14 | −12.01 | −36.52 | 24.50 | 0.45 | 3.14 | 7.29 | −4.15 | −0.08 |
| Annual | −13.26 | −59.55 | −8.23 | −35.46 | 27.23 | 0.50 | 3.08 | 5.91 | −2.83 | −0.05 |
| Gandhi College | | | | | | | | | | |
| Winter | −15.86 | −48.49 | −11.73 | −35.78 | 24.05 | 0.45 | 1.89 | 4.21 | −2.32 | −0.04 |
| Premonsoon | −12.67 | −68.38 | −7.47 | −41.59 | 34.11 | 0.63 | 3.77 | 6.32 | −2.55 | −0.05 |
| Monsoon | −14.89 | −55.03 | −8.83 | −32.51 | 23.69 | 0.44 | 2.81 | 2.83 | −0.02 | −0.01 |
| Postmonsoon | −15.70 | −50.02 | −10.86 | −35.07 | 24.21 | 0.45 | 1.78 | 3.27 | −1.49 | −0.03 |
| Annual | −14.78 | −55.48 | −9.72 | −36.24 | 26.52 | 0.49 | 2.56 | 4.16 | −1.59 | −0.03 |

Seasonal and annual mean shortwave aerosol radiative forcing efficiency at TOA and SFC are also given
*TOA* top of the atmosphere, *SFC* surface, *ATM* atmosphere, *HR* heating rate

when compared to Gandhi College despite a relatively higher surface albedo (Table 1); AODs are comparable over Kanpur and Gandhi College during postmonsoon; however, SSA is higher over Kanpur. The higher SSA overwhelms the surface albedo effect over Kanpur and gives rise to a more negative TOA forcing. Similar phenomenon occurs during premonsoon over Gandhi College when SSA is higher than Kanpur and TOA forcing is more negative (Table 6) while the surface forcing is comparable between Kanpur and Gandhi College.

### 4.2 Effect of curvature in aerosol optical depth spectra on shortwave radiative effects

When the aerosol size distribution is multimodal, the wavelength dependence of AOD does not follow Ångström power law and shows departure from the linear behavior of ln AOD versus ln λ (Eck et al. 2001). The second-order polynomial fit to examine the curvature in the AOD spectra can be written as $\ln\tau = \alpha_2(\ln\lambda)^2 + \alpha_1\ln\lambda + \alpha_0$, where $\alpha_0$, $\alpha_1$ and $\alpha_2$ are constants. Coefficient $\alpha_2$ represents the curvature observed in the spectral distribution of AODs. $\alpha_2$ is $<$ 0 when fine mode particles dominate the aerosol size distribution, and $\alpha_2$ is $>$ 0 when coarse mode aerosols are dominant or the aerosol size distribution is bimodal with significant relative magnitude of coarse mode particles (Eck et al. 2001). Curvatures in AOD spectra can modify the aerosol optical properties (Eck et al. 2001). In the present study, the influence of curvature in spectral AODs on aerosol radiative forcing is examined over Kanpur and Gandhi College, where AODs are higher than 0.85 at 0.5 μm (Fig. 3). $\alpha_2$ values are −0.69 (November) and −0.58 (December) over Kanpur and Gandhi College, respectively. Owing to the presence of curvature in the spectral distribution of AODs, ARF is lower (case 2, Fig. 3) as the AODs are lower when compared to the ARF obtained without including the curvature effects (case 1), thus suggesting that curvatures in the spectral distribution of AODs can reduce ARF significantly (≥10%).

### 4.3 Longwave and net aerosol radiative forcing

Longwave (4.0–40.0 μm) ARF for different seasons over Kanpur and Gandhi College are shown in Fig. 4. Longwave surface forcing is positive in contrast to the shortwave forcing. The longwave impact of aerosols can be either positive or negative on the atmosphere (Ramaswamy 2002); longwave absorption by aerosols cool the atmosphere (Fig. 4). The infrared absorption by aerosols decrease the outgoing longwave flux while increasing the surface reaching infrared radiation which results in a cooling of the atmosphere. The magnitude of longwave forcing and the cooling is significantly small when compared to the shortwave, and in terms of absolute magnitude, the longwave contributes only about 20% or less to the net forcing (Figs. 2, 4 and 5). The contribution of longwave to the net (shortwave + longwave) ARF over Kanpur and Gandhi College is higher than those reported earlier over Ahmedabad (Ramachandran and Kedia 2010), an urban location in western India, and Hisar

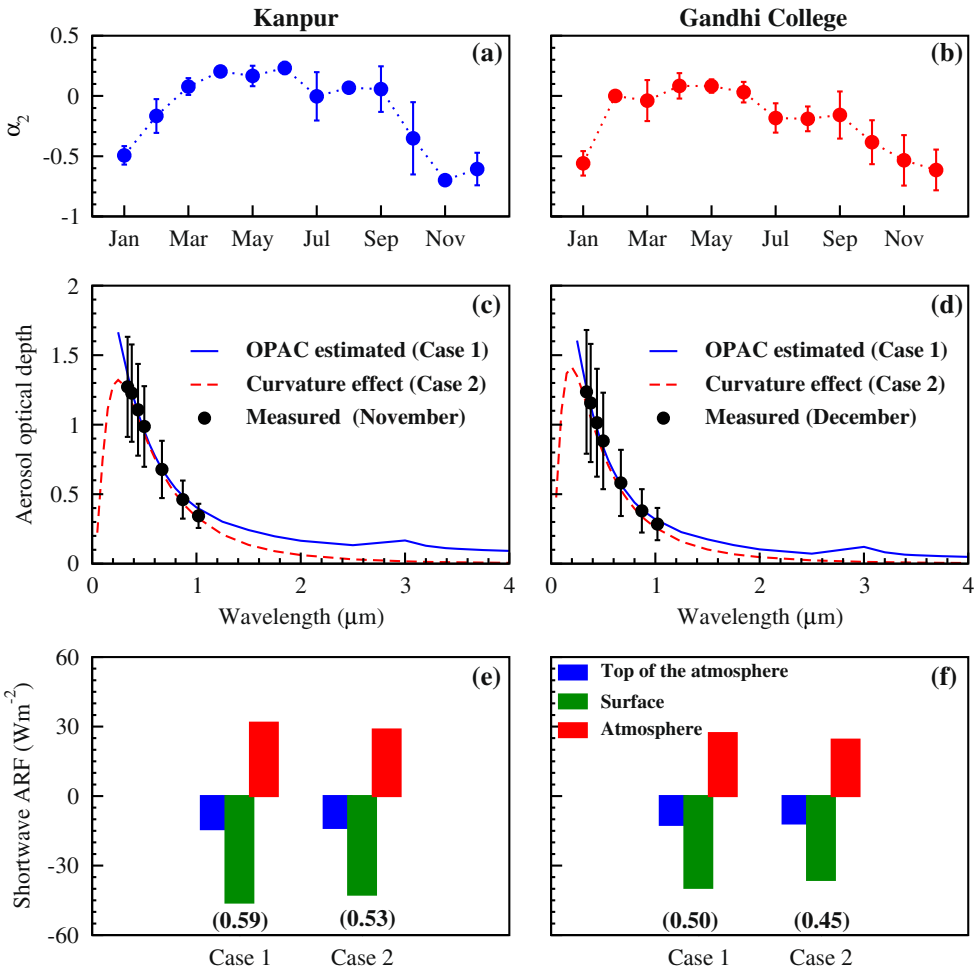


**Fig. 3** Monthly mean variation in $\alpha_2$ (measure of curvature in AOD spectra) over **a** Kanpur and **b** Gandhi College during 2006–2008. Measured aerosol optical depth spectra in comparison with OPAC estimated AOD spectra over **c** Kanpur and **d** Gandhi College. *Vertical bars* indicate $\pm 1\sigma$ deviation from the mean. AOD spectra determined including curvature effects are also shown. ARF determined over **e** Kanpur and **f** Gandhi College for both cases: case 1 (OPAC estimated) and case 2 (curvature effect). Atmospheric heating rates (kelvin per day) for both cases are given in *brackets*

(Ramachandran et al. 2006), a semi-urban location in northern India. Longwave ATM forcing is less negative during monsoon over Kanpur and Gandhi College (Fig. 4). The contribution of longwave ARF to the net ARF increases when AOD increases. For example, in absolute magnitude longwave contribution to ATM forcing is <1% in Gandhi College during monsoon which increases to 11% during winter; AOD increases from 0.59 (monsoon) to 0.74 in winter, while SSA decreases. SSA of different aerosol species are substantially low in the infrared indicating significant absorption in the longwave (Ramachandran et al. 2006). The results indicate that the contribution of longwave to the net ARF can increase in a turbid atmosphere comprising abundant absorbing aerosols. Longwave heating rate is higher over Kanpur when compared to Gandhi College except during winter (Table 6). This is attributed to the higher abundance of coarse mode (dust) aerosols over Kanpur when compared to Gandhi College (Table 2).

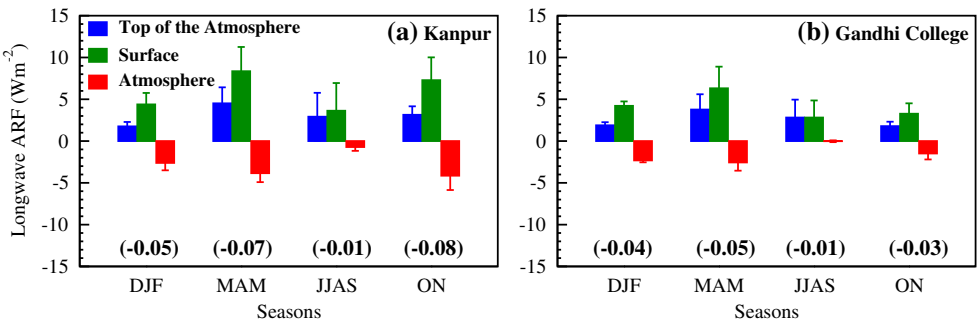


**Fig. 4** Seasonal variation in longwave ARF at the top of the atmosphere, surface and in the atmosphere estimated for **a** Kanpur and **b** Gandhi College. *Vertical bars* indicate $\pm 1\sigma$ variation from the mean. The longwave heating rates (kelvin per day) are given in *brackets*

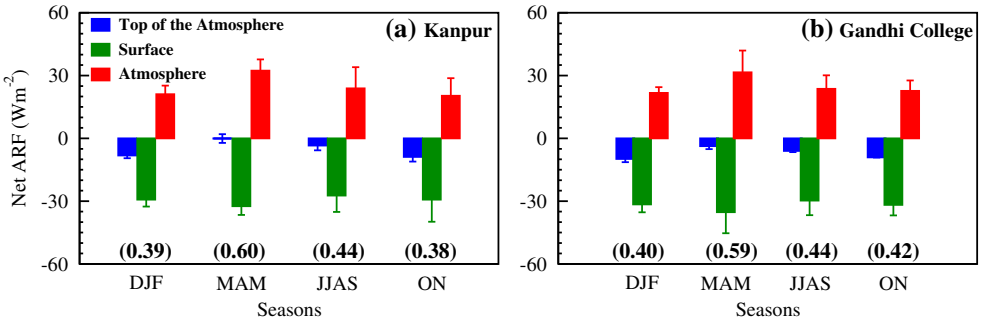


**Fig. 5** Seasonal variation in net (shortwave + longwave) ARF at the top of the atmosphere, surface and in the atmosphere estimated for **a** Kanpur and **b** Gandhi College. *Vertical bars* indicate $\pm 1\sigma$ variation from the mean. The net (shortwave + longwave) heating rates (kelvin per day) are given in *brackets*

### 4.4 Implications

It is clear from the results on aerosol radiative effects over Kanpur and Gandhi College that despite differences in aerosol characteristics owing to the dominance of different aerosol types and sizes, the radiative effects are of similar magnitude (Figs. 2, 4 and 5; Tables 2 and 6). ARFE at TOA and SFC exhibit strong seasonal differences over Kanpur and Gandhi College. This occurs due to the seasonal differences in aerosol and surface reflectance characteristics. ARFE is the highest over the Indo-Gangetic Plain during premonsoon when surface reflectance is higher and SSA is lower. In Kanpur, despite similar SSA during winter and monsoon, ARFE at TOA is less negative in monsoon and ARFE at SFC is the highest owing to higher surface albedo. Similar differences are seen between premonsoon and postmonsoon over Gandhi College. Results suggest that when surface albedo is higher, aerosol radiative effects can be more stronger when aerosols of absorbing nature are abundant. High values of ARF over a large spatial domain (IGP) confirms that although aerosols are abundant near source regions, they can impact regional and global climate as they and their radiative influence can get transported due to atmospheric circulation patterns. ARF at the surface and TOA for the Indo-Asian region corresponding to January–April (Preindustrial to 1996–1999) period was reported to be $-14 \pm 3$ and $0 \pm 2$ W m$^{-2}$, respectively (Ramanathan et al. 2001), resulting in an atmospheric warming of $14 \pm 3$ W m$^{-2}$ due to aerosols. Greenhouse gas forcing for the same period and the region was estimated to be 1, 1.6 and 2.6 W m$^{-2}$ at SFC, in the atmosphere and TOA, respectively (Ramanathan et al. 2001). ARF at the surface and atmospheric warming over Kanpur and Gandhi College in the IGP throughout the year are at least two to three times higher than those reported for the Indo-Asian region for January–April and is more than an order of magnitude higher when compared to greenhouse gas forcing. Such large atmospheric heating and surface forcing due to aerosols on a regional scale can have significant influence on atmospheric stability and cloud formation in the tropics (Menon et al. 2002) and can affect the precipitation and hydrological cycle (Ramanathan et al. 2001). A large atmospheric warming over IGP (>0.6 K/day) becomes important in the context of the elevated heat pump hypothesis (Lau and Kim 2006) where in the large premonsoon, atmospheric warming due to aerosols can influence the amount of rainfall and advance of the monsoon season over India. Thus, such large atmospheric heating over IGP and its interannual variation not only can have adverse impact on monsoon and rainfall trends (Gautam et al. 2009) but also on agriculture (Auffhammer et al. 2006). The study highlights the presence of a large atmospheric warming due to aerosols on a regional scale throughout the year and its potential impact on climate and agriculture, which are important and need to be assessed in greater detail with measurements and data.

## 5 Summary and conclusions

Seasonal variation in aerosol radiative effects have been investigated for the first time over two environmentally distinct locations, Kanpur (urban site) and Gandhi College (rural location) in the Indo-Gangetic plain, a regional aerosol hot spot, utilizing the measured spectral aerosol properties (AOD, SSA and asymmetry parameter ($g$), an aerosol optical properties model and a radiative transfer model. The possible climate implications are presented.

The major conclusions from the study are summarized as follows:

1. Aerosol radiative forcing estimated using optical properties model and a radiative transfer model is found to be in good agreement with AERONET retrieved aerosol radiative forcing, thus emphasizing that the approach adopted to retrieve the spectral aerosol optical properties and further to derive aerosol radiative forcing is robust.

A good agreement between model estimates and AERONET forcing indicates that the inversion problem of the retrieval of aerosol properties using various aerosol components is well constrained for the solution of the inversion problem to be unique.

2. Aerosol radiative forcing efficiency at the TOA and at the SFC exhibit large seasonal differences because of differences in aerosol characteristics and surface reflectance. Aerosol radiative forcing efficiency at TOA is found to be less negative during premonsoon, while the efficiency at the surface is more negative due to higher surface albedo.
3. Shortwave aerosol radiative forcing at TOA is negative ($\leq -12$ W m$^{-2}$) throughout the year over Kanpur and Gandhi College. Aerosol forcing at the surface is $\geq -30$W m$^{-2}$. Atmospheric warming is maximum during premonsoon ($>30$ W m$^{-2}$), as the difference between TOA and SFC forcing is maximum during premonsoon. Solar atmospheric heating rate is $\geq$0.4 K/day over Kanpur and Gandhi College and peaks at $>$0.6 K/day during premonsoon which is attributed to lower SSA ($<$0.9) and higher surface albedo ($>$0.1).
4. TOA forcing is always less negative over Kanpur when compared to Gandhi College due to lower surface albedo. TOA forcing is more negative during postmonsoon over Kanpur due to higher SSA. This is because surface ARF is linearly related to AODs, while TOA forcing depends on SSA and surface albedo in addition to AOD.
5. The presence of curvature in the spectral distribution of AODs, when AODs are higher, can modify ARF significantly ($\geq$10%).
6. Aerosols can cause a cooling of the atmosphere in the longwave. The magnitude of longwave forcing and atmospheric cooling in an absolute sense is significantly small and contributes only about 20% or less to the net (shortwave + longwave) forcing. The percentage contribution of longwave forcing to the net forcing increases when AODs are higher.
7. Aerosol radiative effects over Kanpur and Gandhi College, despite differences in aerosol characteristics are similar and high, thus confirming that aerosols can impact regional and global climate as their radiative influence gets transported due to atmospheric circulation.
8. The atmospheric warming and the reduction of solar irradiance at the surface due to aerosols in two locations, Kanpur and Gandhi College, separated by about 300 km, over a large spatial domain are at least an order of magnitude higher when compared to the greenhouse gas forcing. Such large regional imbalance in the Earth–atmosphere radiation budget can have implications on agriculture, cloud formation, precipitation and hydrological cycle and should be taken into account while conducting regional-scale assessments of climate impact.

**Acknowledgements** We thank B. N. Holben, R. P. Singh and S.N. Tripathi for their efforts in establishing and maintaining the AERONET sun/sky radiometers at Kanpur and Gandhi College, the data of which are used to estimate aerosol radiative forcing reported in the study. Temperature, pressure and relative humidity are obtained from NCEP Reanalysis. Columnar ozone and water vapor are downloaded from GES-DISC, NASA.

## References

Andrews E, Sheridan PJ, Fiebig M, McComiskey A (2006) Ogren JA, Arnott P, Covert D, Elleman R, Gasparini R, Collins D, Jonsson H, Schmid B, Wang J (2006) Comparison of methods for deriving aerosol asymmetry parameter. J Geophys Res 111:D05S04. doi:10.1029/2004JD005734

Auffhammer M, Ramanathan V, Vincent JR (2006) Integrated model shows that atmospheric brown clouds and greenhouse gases have reduced rice harvests in India. Proc Natl Acad Sci 103:19668–19672

Dey S, Tripathi SN (2008) Aerosol direct radiative effects over Kanpur in the Indo-Gangetic basin, northern India: long-term (2001–2005) observations and implications to regional climate. J Geophys Res 113:D04212. doi:10.1029/2007JD009029

Dubovik O, King MD (2000) A flexible inversion algorithm for retrieval of aerosol optical properties from Sun and sky radiance measurements. J Geophys Res 105:20673–20696

Dubuisson P, Buriez JC, Fouquart Y (1996) High spectral resolution solar radiative transfer in absorbing and scattering media: application to the satellite simulation. J Quant Spectrosc Radiat Transfer 55:103–126

Eck TF, Holben BN, Dubovik O, Smirnov A, Slutsker I, Lobert JM, Ramanathan V (2001) Column-integrated aerosol optical properties over the Maldives during the northeast monsoon for 1998–2000. J Geophys Res 106:28555-28566

Gautam R, Hsu NC, Lau, K-M, Katafos M (2009) Aerosol and rainfall variability over the Indian monsoon region: distributions, trends and coupling. Ann Geophys 27:3691–3703

Hess M, Koepke P, Schult I (1998) Optical properties of aerosols and clouds: the software package OPAC. Bull Am Meteorol Soc 79:931–844

Lau K-M, Kim K-M (2006) Observational relationships between aerosol and Asian monsoon rainfall, and circulation. Geophys Res Lett 33:L21810. doi:10.1029/2006GL027546

Liou KN (1980) An introduction to atmospheric radiation, 392 pp. Academic, San Diego

Menon S, Hansen J, Nazarenko L, Luo Y (2002) Climate effects of black carbon aerosols in China and India. Science 297:2250–2253

Michalsky JJ, Anderson GP, Barnard J, Delamere J, Gueymard C, Kato S, Kiedron P, McComiskey A, Ricchiazzi P (2006) Shortwave radiation closure studies for clear skies during the atmospheric radiation measurement 2003 aerosol

intensive observation period. J Geophys Res 111:D14S90. doi:10.1029/2005JD006341

Mishchenko MI, Travis LD, Kahn RA, West RA (1997) Modeling phase functions for dustlike tropospheric aerosols using a shape mixture of randomly oriented polydisperse spheroids. J Geophys Res 102:16831–16847

Ramachandran S, Rengarajan R, Jayaraman A, Sarin MM, Das SK (2006) Aerosol radiative forcing during clear, hazy, and foggy conditions over a continental polluted location in north India. J Geophys Res 111:D20214. doi:10.1029/2006JD007142

Ramachandran S, Cherian R (2008) Regional and seasonal variations in aerosol optical characteristics and their frequency distributions over India during 2001–2005. J Geophys Res 113:D08207. doi:10.1029/2007JD008560

Ramachandran S, Kedia S (2010) Black carbon aerosols over an urban region: radiative forcing and climate impact. J Geophys Res 115:D10202. doi:10.1029/2009JD013560

Ramanathan V, Crutzen P, Kiehl JT, Rosenfeld D (2001) Aerosols, climate and the hydrological cycle. Science 294:2219–2224

Ramaswamy V (2002) Infrared radiation in encyclopedia of global environmental change, vol I, pp 470–475. Wiley, Hoboken

Ricchiazzi P, Yang S, Gautier C, Sowle D (1998) SBDART, a research and teaching tool for plane-parallel radiative transfer in the Earth's atmosphere. Bull Am Meteorol Soc 79:2101–2114

Singh RP, Dey S, Tripathi SN, Tare V, Holben B (2004) Variability of aerosol parameters over Kanpur, northern India. J Geophys Res 109:D23206. doi:10.1029/2004JD004966

Solomon S, Qin D, Manning M, Chen Z, Marquis M, Averyt KB, Tignor M, Miller HL (eds) (2007) Summary for policymakers, intergovernmental panel on climate change, 142 pp. Cambridge University Press, Cambridge

Srivastava AK, Tiwari S, Devara PCS, Bisht DS, Srivastava MK, Tripathi SN, Goloub P, Holben BN (2011) Pre-monsoon aerosol characteristics over the Indo-Gangetic basin: implications to climatic impact. Ann Geophys 29:789–804

Stull RB (1988) An introduction to boundary layer meteorology, 666 pp. Kluwer Academic, Dordrecht